Study on Effect of Junction Temperature Swing Duration on Lifetime of Transfer Molded Power IGBT Modules

Ui-Min Choi, *Member, IEEE*, Frede Blaabjerg, *Fellow, IEEE*, and Søren Jørgensen

***Abstract*—In this paper, the effect of junction temperature swing duration on lifetime of transfer molded power insulated gate bipolar transistor (IGBT) modules is studied and a relevant lifetime factor is modeled. This study is based on 39 accelerated power cycling test results under six different conditions by an advanced power cycling test setup, which allows tested modules to be operated under more realistic electrical conditions during the power cycling test. The analysis of the test results and the temperature swing duration dependent lifetime factor under different definitions and confidence levels are presented. This study enables to include the $t_{\triangle \mathrm{Tj}}$ effect on lifetime model of IGBT modules for its lifetime estimation and it may result in improved lifetime prediction of IGBT modules under given mission profiles of converters. A postfailure analysis of the tested IGBT modules is also performed.**

***Index Terms*—Failure mechanism, insulated gate bipolar transistor (IGBT), IGBT module, junction temperature swing duration, lifetime model, power cycling test, reliability.**

I. Introduction

POWER semiconductor devices are one of the most reliability-critical components and thus play a key role in the robustness and reliability of overall power electronic systems [1]–[3]. In practical applications, power devices are used in a form of package such as discrete devices and modules, due to several reasons [4]. Insulated gate bipolar transistor (IGBT) power modules are the most widely used of their kind in power ranges from several hundred W to several MW [4]. Thermo-mechanical stress is generally the main cause of degradation of IGBT modules [4]–[7]. Therefore, much research has been devoted to the reliability of power IGBT modules in respect to temperature stress such as evaluation of new device packaging materials and designs, failure mechanism analysis, lifetime modeling and estimation [8]–[10].

The lifetime modeling of IGBT modules in respect to temperature stress is one of the important topics in the reliability research. From a lifetime model, the lifetime of IGBT modules can be estimated under given mission profiles of power converters [11]. Further, it can be used for design for reliability in order to achieve the required reliability and robustness of power electronic products with reduced cost [10]. A lifetime model is developed based on the power cycling test results in respect to temperature stress factors such as junction temperature swing ($\triangle T_j$) and mean junction temperature (T_{jm}) [12]–[14]. In temperature stress factors, not only the junction temperature swing ($\triangle T_j$) and mean junction temperature (T_{jm}) but also the temperature swing duration ($t_{\triangle Tj}$) is an important factor from a real application point of view. While the impacts of $\triangle T_j$ and T_{jm} on lifetime of IGBT modules are well investigated by prior art researches but there is still a lack of quantitative study on the effect of $t_{\triangle Tj}$.

In recent research [15], [16], the impact of load pulse duration on power cycling lifetime has been investigated for solder-free power modules based on DC power cycling test and the related lifetime model has been formed. It has been concluded that the load pulse duration has a significant impact on the power cycling lifetime of IGBT modules. Further, in [17], the lifetime model has been developed including effect of power on time (t_{on}), which is somewhat similar parameter with load pulse duration, based on the test data. However, these kinds of prior art researches have some limitations that the detailed testing data are not available and the defined lifetime criteria and confidence level of a specific lifetime model are not usually provided. Moreover, corresponding postfailure analysis is also not provided. In addition, in the DC power cycling test, the tested module is not operated under realistic electrical conditions. The temperature of the tested module increases by only conduction loss. If the temperature is reached to the desired maximum temperature, the applied power is disconnected and the temperature is decreased by the external cooling system. This period (T_s) is defined as cycle and it is repeated until the tested module is failed. The duration and amplitude of the current pulse are changed in order to obtain the specific junction temperature swing $\triangle T_j$ and mean junction temperature T_{jm}. Therefore, there are no switching of device under test (DUT), no dynamic loss and high DC-link voltage, etc. [6]. Further, an overload current may be required for high temperature swing in a short period. In [16], there is a large error in the verification of the load pulse duration impact with a real power converter. Therefore, more improved research considering the above limitations is still required.

In his paper, the effect of junction temperature swing duration on the lifetime of an IGBT module is studied with 600 V, 30 A,

Manuscript received July 4, 2016; revised August 27, 2016; accepted October 6, 2016. Date of publication January 17, 2017; date of current version March 24, 2017. Recommended for publication by Associate Editor J. Wang.

U.-M. Choi and F. Blaabjerg are with the Energy Technology, Aalborg University, Aalborg 9220, Denmark (e-mail: uch@et.aau.dk; fbl@et.aau.dk).

S. Jørgensen is with the Grundfos Holding A/S, Bjerringbro DK-8850, Denmark (e-mail: soejoergensen@grundfos.com).

Color versions of one or more of the figures in this paper are available online at http://ieeexplore.ieee.org

Digital Object Identifier 10.1109/TPEL.2016.2618917

three-phase transfer molded intelligent power IGBT modules (IPM). This study is based on power cycling test results with 39 samples under six test conditions by the advanced power cycling test setup, which allows IGBT module being operated under more realistic electrical conditions of the converters. This paper starts with the basic statistics for lifetime analysis and modeling.

Then, the power cycling test setup, IGBT module under test and test conditions are described. Detailed lifetime analysis with different lifetime definitions and confidence levels are provided and a relevant lifetime factor is modeled based on test results. Finally, postfailure analysis results of the tested IGBT modules by scanning electron microscopy (SEM) and scanning acoustic microscopy (SAM) are also presented.

II. Weibull Analysis and Test Sample Size

Reliability is defined as the ability of an item to perform the required function under stated conditions for a certain period of time [1]. The reliability is typically represented by the probability of survival and failure rate because it is influenced by variability such as variations in manufacturing process, environments, and other varying factors. Therefore, in reliability modeling, the statistical data analysis is an essential part in order to deal with uncertainties.

A. Weibull Distribution

A Weibull distribution, especially suited for the description of end-of-life phenomena, is a popular distribution in reliability engineering for analyzing life data. The cumulative failure distribution function *F(t)* is defined as [18]

$$F(t) = 1 - \exp\left[-\left(\frac{t - t_0}{\eta - t_0}\right)\right]^{\beta} \tag{1}$$

where F is the probability of failure, t is the test statistic (time or number of cycles), t_0 is the minimum life (failure free period or number of cycles), β is the Weibull slope or shape parameter, and η is the characteristic life (where $F = 63.2\%$ or it is also called the scale parameter).

B. Test Sample Size

As mentioned above, in reliability engineering, the statistical data are essential and it can be expected to obtain more accurate results as a sample size for the test is larger. However, there is a limitation in sample size due to reasons such as cost and time for reliability tests.

In this situation, the data ranking is a good solution for the compensation of small sample size because it provides an estimate of what percentage of population is represented by the particular test sample.

Median Rank (MR) is one of the most used methods for probability plotting in reliability engineering. It is defined as a cumulative percentage of the population represented by a particular sample with 50% confidence level and can be calculated simply by the Benard's approximation [18]. The MR is approximately calculated as

$$\text{MR}\,(\%) = \left(\frac{j - 0.3}{N + 0.4}\right) \times 100 \tag{2}$$

where j is the failure order number and N is the sample size.

TABLE I
MR of Each Sample According to Sample Size (Value is Given in Percentage)

	Sample size									
Rank order	1	2	3	4	5	6	7	8	9	10
1	50.00	29.16	20.58	15.91	12.96	10.93	9.46	8.33	7.45	6.73
2		70.83	50.00	38.63	31.48	26.56	22.97	20.23	18.08	16.35
3			79.41	61.36	50.00	42.18	36.48	32.14	28.72	25.96
4				84.09	68.52	57.81	50.00	44.04	39.36	35.58
5					87.03	73.43	63.51	55.95	50.00	45.19
6						89.06	77.02	67.86	60.64	54.81
7							90.54	79.76	71.28	64.42
8								91.67	81.91	74.03
9									92.55	83.65
10										93.27

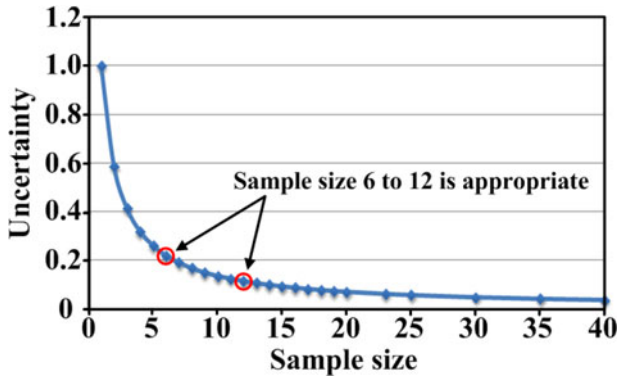

Fig. 1. Uncertainty versus sample size in Weibull plotting.

Table I shows the MR of each sample according to the sample size. For example, MR of second-order sample out of six samples, those two samples represent 26.56% of the total population with 50% confidence.

From the MR, the uncertainty can be calculated as

$$\text{Uncertainty} = 1 - \left(MR_{\text{\_higest}(\%)} - MR_{\text{\_lowest}(\%)}\right) \tag{3}$$

where MR_higest and MR_lowest are the highest and lowest MRs, respectively, for a given sample size.

Fig. 1 shows the uncertainty according the sample size. A sample size of 6 is down in the knee of the curve and the sample size of 12 is beyond the knee of the curve.

It can be seen that 6–12 samples would be appropriate for the test. Therefore, in this paper, the minimum sample size of 6 is chosen for the power cycling test.

III. Accelerated Power Cycling Test Under Different Junction Temperature Swing Durations ($t_{\triangle T_j}$)

A. Power Cycling Test Setup and DUT

1) Advanced Power Cycling Test Setup: Fig. 2 shows a configuration of an advanced accelerated power cycling test setup.

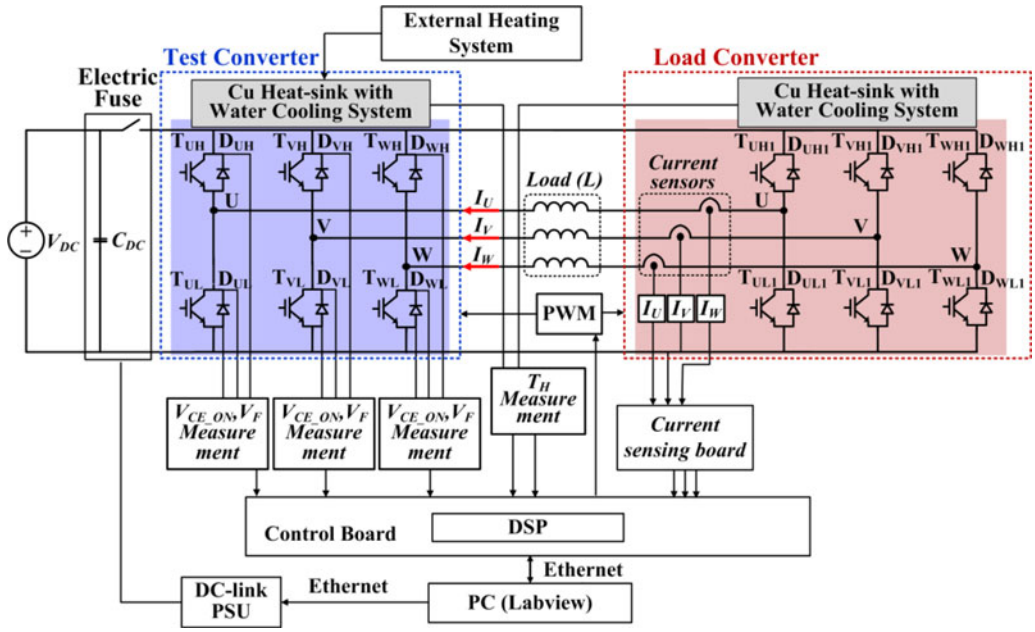

Fig. 2. Configuration of an advanced accelerated power cycling test setup.

Two three-phase converters are connected through load inductors. One is a test converter with the IGBT module under test and the other one is a load converter. In the load converter, an IGBT module that has a higher rated power than the tested module is used so that the load converter can run for a long time even though the tested IGBT modules are changed after a certain number of power cycling tests by reducing the effect of the thermal stresses on the load IGBT module during accelerated power cycling tests. These two converters are connected with a DC source ($V_{\rm DC}$) via an electric fuse (see Fig. 2) in order to protect the overall system under abnormal operations of the test setup. The on-state collector–emitter voltages ($V_{\rm CE\_ON}$) of IGBTs and forward voltages (V_F) of the diodes are measured in real time by an online $V_{\rm CE\_ON}$ measurement circuit to monitor the wear-out condition of the IGBT module under the test. The two converters are controlled by a control board with a digital signal processor (DSP) and Labview interface communicates with a DSP to manage and monitor the overall system and also saves the values of monitoring parameters. A water cooling system and external temperature controllable heater system are used in order to change the heat-sink temperature depending on the desired test conditions and in order to keep the heat-sink temperature of the tested module as a constant during power cycling tests.

The main advantages of this test setup are the following. First, the accelerated power cycling tests can be performed under more realistic electrical conditions close to real three-phase converter applications such as in motor and grid-connected systems compared with conventional DC power cycling test. Second, it is easily possible to apply various thermal stress conditions in a short cycle period by changing the various parameters such as switching frequency, output frequency, modulation index, power

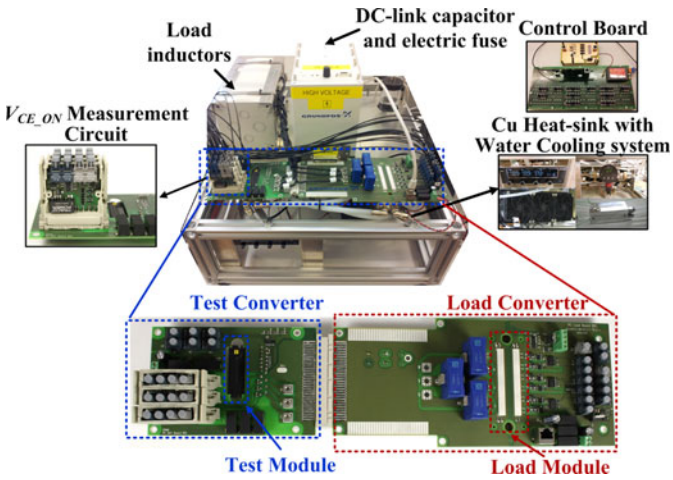

Fig. 3. Prototype of the power cycling test setup.

factor, and magnitudes of output current and voltage. Further, the wear-out condition of the tested power module can be monitored in real time, which gives a convenience to perform the test. Finally, the power consumption during power cycling tests can be kept low because the generated power is circulated between two converters. It means that there are only losses by two IGBT modules and load inductors. Thus, it is a cost-effective solution compared to power cycling test with real loads [19].

Fig. 3 shows a prototype of the advanced accelerated power cycling test setup. In this system, a 600 V, 30 A, three-phase transfer molded IPM is used for the test converter and a 1200 V, 75 A, three-phase IGBT module is used for the load converter. More detailed information about the test setup can be obtained in [12] and [23].

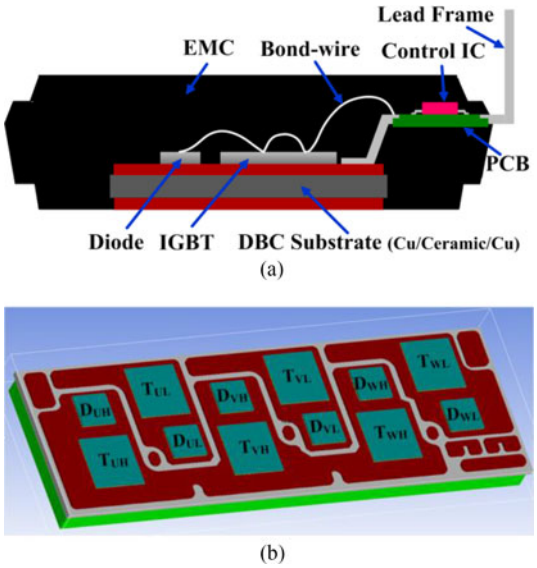

Fig. 4. Transfer molded IPM. (a) Vertical structure. (b) Configuration of power devices with six IGBTs (*T*) and six diodes (*D*).

2) Power IGBT Module Under Test: Fig. 4(a) shows a vertical structure and configuration of the 600 V, 30 A, three-phase transfer molded IPM. The IPM consists of six IGBTs and six diodes and they are mounted on a direct bonded copper (DBC) substrate with aluminum wire interconnection. The lead frame is connected to the DBC substrate by soldering and a copper surface of the DBC substrate is exposed to be contacted with an external heat sink. Further, controlled integrated circuits for gate driving are embedded inside the module too. This module is covered by epoxy molding compound and does not have a base plate. Fig. 4(b) shows the configuration of the IPM. Due to mainly smaller die size, diodes have larger thermal impedance than that of IGBTs. However, in this test, the tested IGBT module is operated under inverter mode with unity power factor and thus losses in IGBTs are dominant. Therefore, IGBTs have higher junction temperature and larger junction temperature variation than diodes. T_{VL} in Fig. 4(b) is considered as the standard device for finding the conditions because it has the highest thermal impedance among IGBTs because of asymmetric packaging layout and thus has the highest temperature stress in this module [11].

B. Test Conditions

Six test conditions are validated by measuring the temperature of an open module covered by black paint using a high-resolution infrared camera (FLIR X8400sc) to study the $t_{\triangle Tj}$ impact on lifetime on the IPM.

Table II shows the six different test conditions. They have almost the same $\triangle T_j$ and T_{jm} (about 81 °C and 102 °C, respectively) but different $t_{\triangle Tj}$ from 0.59 to 10 s in order to clearly study $t_{\triangle Tj}$ impact on the lifetime of IGBT module.

All conditions are in the safe operating area (SOA) of the test device in order to avoid the other failure mechanisms that could come from the operation outside of the SOA.

TABLE II
TEST CONDITIONS FOR THE POWER CYCLING TESTS

Cond.	$t_{\triangle Tj}$ (s)	f_{out} (Hz)	f_{SW} (kHz)	I_{peak} (A)	V_{ref} (V)	T_H (°C)	$\triangle T_j$ (°C)	T_{jm} (°C)
1	10	0.1	10	21	113	59	80.8	102.3
2	5	0.2	10	22	116	57	80.6	102.5
3	2	0.5	10	25	145	53	82.0	101.3
4	1	1	10	30	140	48	81.6	101.5
5	0.8	1.25	12	30	140	50	81.8	102.4
6	0.59	1.7	15	30	143	48	80.8	102.0

$t_{\triangle Tj}$: junction temperature swing duration, f_{OUT} : output frequency, f_{SW} : switching frequency, I_{peak} : peak current, V_{ref} : output reference voltage, T_H : heat-sink temperature, $\triangle T_j$: junction temperature swing, T_{jm} : mean temperature.

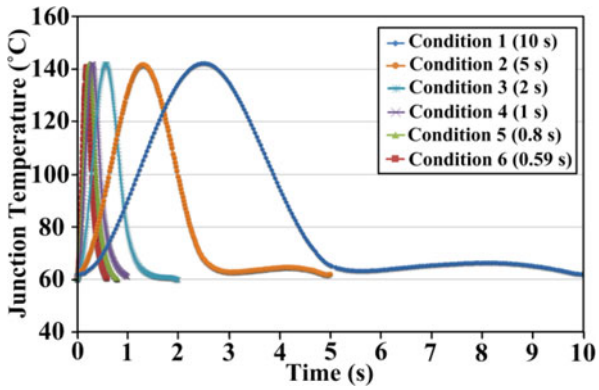

Fig. 5. Temperature profiles under the six operating conditions.

Fig. 5 shows the junction temperature profiles measured by IR camera under the six different test conditions.

C. Power Cycling Test Results Under Different $t_{\triangle Tj}$ Conditions

Six to eight IGBT modules per test condition, totally 39 IGBT modules, are tested. The accelerated power cycling test is stopped if $V_{\mathrm{CE\_ON}}$ increases by 10%–15% from its initial value to protect the tested IGBT modules against catastrophic failure.

Fig. 6 shows the power cycling test results of the six samples under the six conditions. Depending on the testing samples and test conditions, the accelerated power cycling test requires different test periods from 35 to 480 h. For all cases, the wear-out failure occurs first among the low-side IGBTs due to the higher thermal resistance than the high-side IGBTs [12]. The minimum number of cycles to failure per condition is summarized in Table III when the 5% increase of $V_{\mathrm{CE\_ON}}$ is considered as the end of life. As $t_{\triangle Tj}$ increases, the number of cycles to failure decreases. In the case of 10 s, it is about 128900 cycles and it is about 211201 when $t_{\triangle Tj}$ is 0.59 s. Further, among the IGBT modules under the same test conditions, the number of cycles to failure is different to each other from about 20000 to 45000 cycles. As it can be seen from the results, $t_{\triangle Tj}$ has a significant impact on the lifetime of the IGBT modules. Further, a statistical analysis is essentially required because each sample has different lifetime even though they are tested under the same conditions.

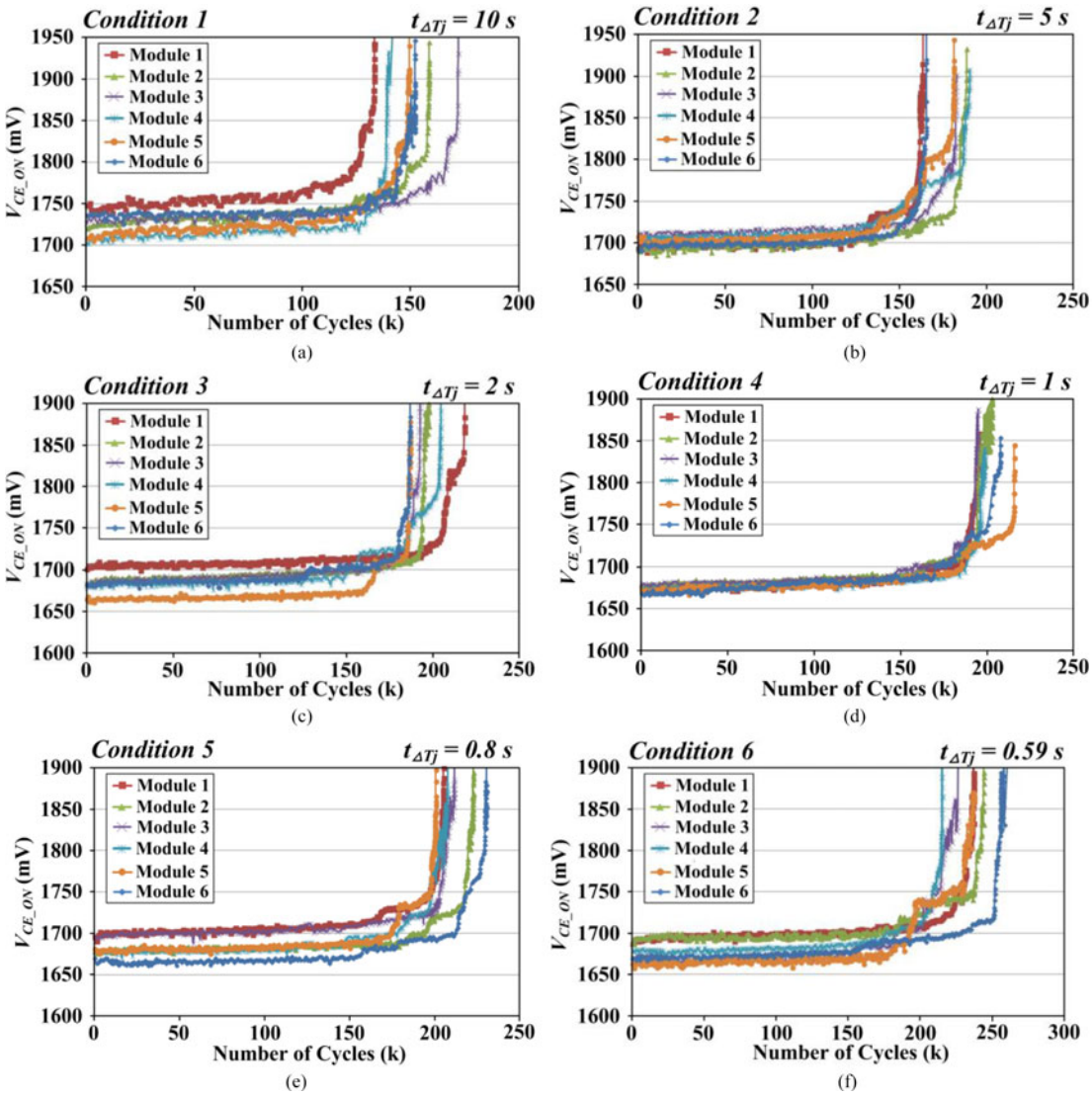

Fig. 6. Power cycling test results under different $t_{\triangle T\,j}$ conditions listed in Table II: (a) condition 1, (b) condition 2, (c) condition 3, (d) condition 4, (e) condition 5, and (f) condition 6.

TABLE III
MINIMUM NUMBER OF CYCLES TO FAILURE UNDER THE TEST CONDITIONS

Condition	$t_{\triangle T\,j}$ (s)	Number of cycles to failure	Test time (h)
1	10	128900	358
2	5	159900	222
3	2	174000	97
4	1	185810	52
5	0.8	197500	44
6	0.59	211201	35

IV. JUNCTION TEMPERATURE SWING DURATION DEPENDENT LIFETIME ANALYSIS BASED ON TEST DATA

The lifetime analysis based on the power cycling test data shown in Section III is discussed. Typically, 5%–20% increase of $V_{\mathrm{CE\_ON}}$ is considered as the end-of-life criterion and the number of cycles until these periods is counted for the lifetime [6]. In this paper, 5% increase of $V_{\mathrm{CE\_ON}}$ is considered as its end-of-life criterion of individual IGBT modules. The time to failure of the tested IGBT modules under the six test conditions are presented by Weibull distribution. The results, shown in Fig. 6, are analyzed using the software tool Weibull++ [20]. The first analysis has been done in [21]. In this paper, one more test result is added and analyzed with new lifetime model.

The lifetime of a population of IGBT modules can be defined with different criteria in terms of time to how much percentage of accumulated failure. For example B_{10} lifetime is the time to 10% of total population is fail. Further, it is important to obtain the predicted lifetime range with a certain confidence boundaries (CB) because the time to failure of each IGBT module varies.

Fig. 7 shows the Weibull plots under the six different conditions with 90% CB. The lifetime with four different definitions with two different confidence levels is summarized in Table IV, where MTTF is mean time to failure. In the case of nominal B_{10} lifetime, the lifetime of six conditions is 127800, 154767, 173938, 183120, 192225 and 205884 cycles, respectively. The lifetime of IGBT modules under the test condition 4 with 90% confidence level is expected within 172551–194337 cycles,

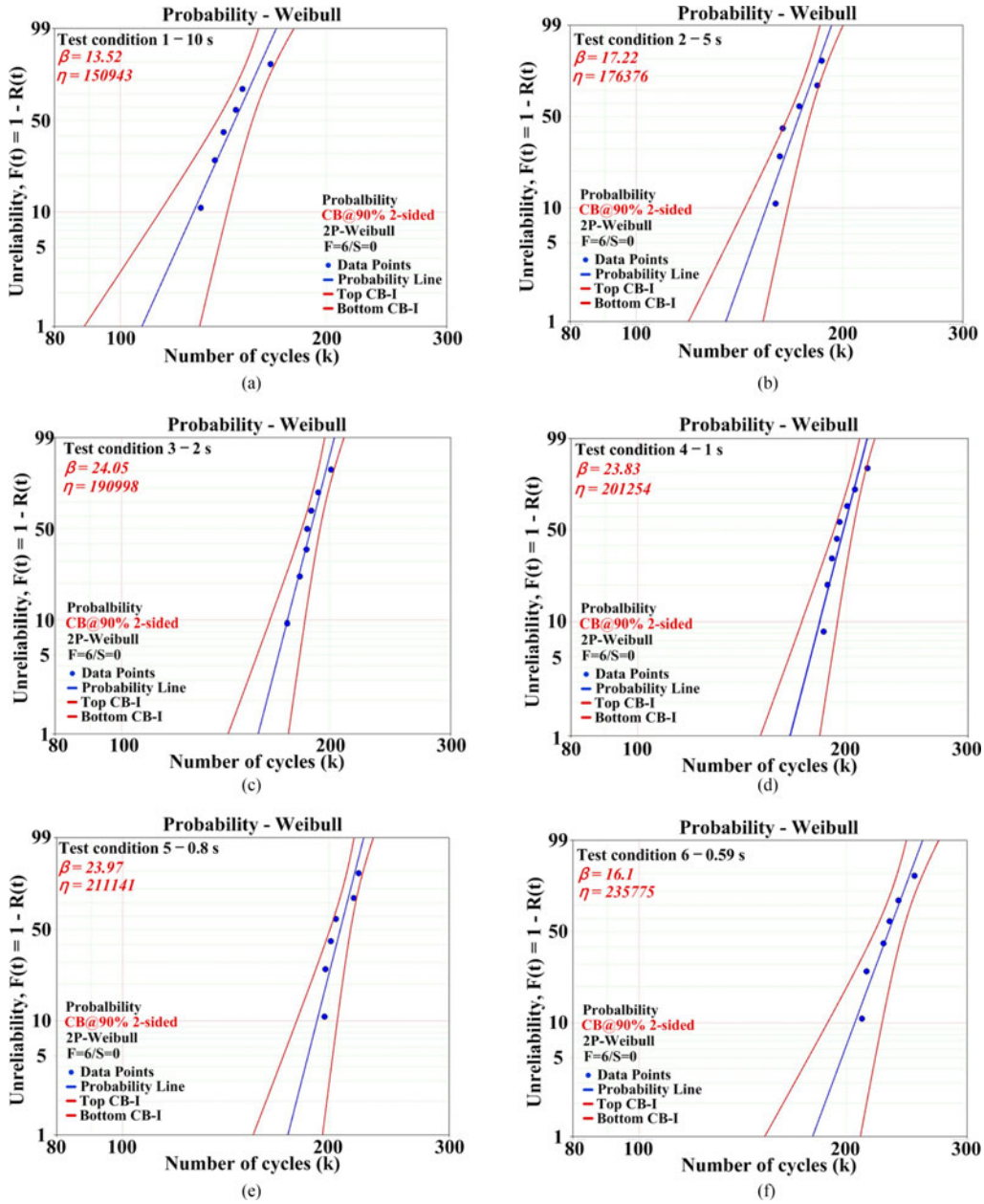

Fig. 7. Lifetime analysis based on power cycling test results in Weibull plots shown in Fig. 6: (a) condition 1, (b) condition 2, (c) condition 3, (d) condition 4, (e) condition 5, and (f) condition 6.

whereas with 99% confidence level, the lifetime range is extended to from 166341 to 200988 cycles. The lifetime under the different definition can also be explained with a similar way.

The effect of $t_{\triangle Tj}$ on the lifetime of the IGBT module can be modeled in the modified form of inverse power law [22] as

$$N_f = \frac{a + b \cdot (t_{\Delta Tj})^{-n}}{a + 1} \tag{4}$$

where N_f is the number of cycles to failure; $t_{\triangle Tj}$ is the temperature swing duration; and a, b, and n are fitting parameters based on test results.

For B_{10} lifetime model, a, b, and n are obtained as –0.989783, 1922.651603, and 0.147656, respectively, based on the nominal lifetime and the corresponding lifetime model for the studied

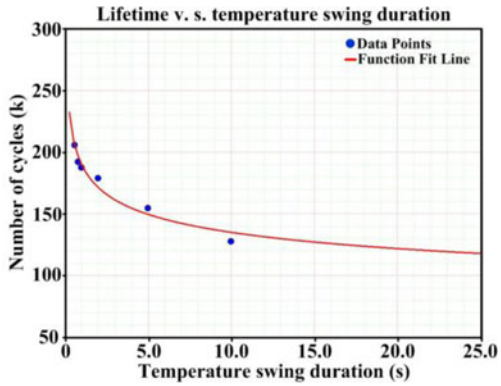

Fig. 8. B_{10} lifetime model for the effect of junction temperature swing duration ($t_{\triangle Tj}$).

TABLE IV
LIFETIME ANALYSIS WITH DIFFERENT DEFINITIONS AND CONFIDENCE LEVELS

Condition		Lifetime (cycles)							
		B_1		B_{10}		$B_{\eta\ (\eta\ =\ 63.2)}$		*MTTF*	
		Confidence level		Confidence level		Confidence level		Confidence level	
		99%	90%	99%	90%	99%	90%	99%	90%
10 s	Bottom CB	79188	88412	106906	114031	138888	143128	131599	136383
	Nominal value	107413		127800		150930		145264	
	Top CB	145697	130497	152777	143231	164036	159176	160348	154724
5 s	Bottom CB	104935	114946	133875	141079	165321	169233	158220	162732
	Nominal value	135025		154767		176372		171021	
	Top CB	173741	158610	178920	169784	188163	183813	184858	179733
2 s	Bottom CB	134696	142611	158694	164043	182961	185825	177443	180745
	Nominal value	157749		173938		190995		186728	
	Top CB	184747	174494	190647	184430	199382	196309	196499	192910
1 s	Bottom CB	142135	150313	166341	172551	192776	195797	186585	190185
	Nominal value	165927		183120		201252		196717	
	Top CB	193700	183163	200988	194337	210100	206858	207400	203473
0.8 s	Bottom CB	145099	155034	172652	179485	201303	204804	194635	198810
	Nominal value	174278		192225		211138		206407	
	Top CB	209323	195910	214015	205868	221454	217669	218892	214295
0.59 s	Bottom CB	138985	152205	178349	187848	220554	225937	211242	217282
	Nominal value	178710		205884		235770		228378	
	Top CB	229788	209830	237670	225652	252036	246031	246905	240042

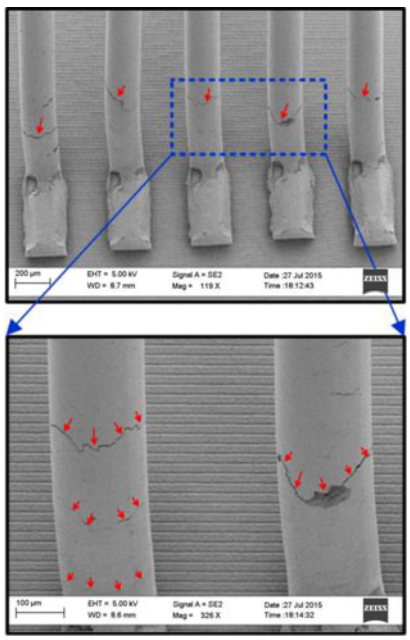

Fig. 9. SEM image of the tested IPM under the condition 4 for the failure analysis.

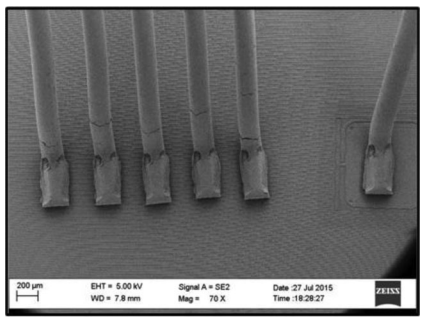

Fig. 10. SEM image of another tested IPM under the condition 4 for the failure analysis.

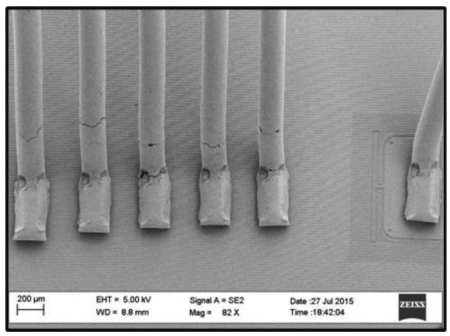

Fig. 11. SEM image of the tested IPM under the condition 1 for the failure analysis.

TABLE V
PARAMETERS OF MODEL (4) UNDER DIFFERENT SELECTED LIFETIME DEFINITIONS

Lifetime	*a*	*b*	*n*
B_1	–0.990124	1653.251685	0.159895
B_{10}	–0.989783	1922.651603	0.147656
B_{20}	–0.989940	1963.800773	0.143583
B_{30}	–0.990089	1979.247972	0.141000
$B_{\eta(=63.2)}$	–0.990281	2043.658801	0.128696
MTTF	–0.990128	1994.791473	0.129448

IGBT module is plotted, as shown in Fig. 8. However, it should be noted that the values of parameters *a*, *b,* and *n* could be varied depending on different lifetime definitions and confidence levels because the IGBT modules have the different number of cycles to failure, as listed in Table IV. For example, B_1 lifetime model, *a*, *b,* and *n* are defined as –0.990124, 1653.251685, and 0.159895, respectively.

Therefore, it is important to know the specific definition of a lifetime model.

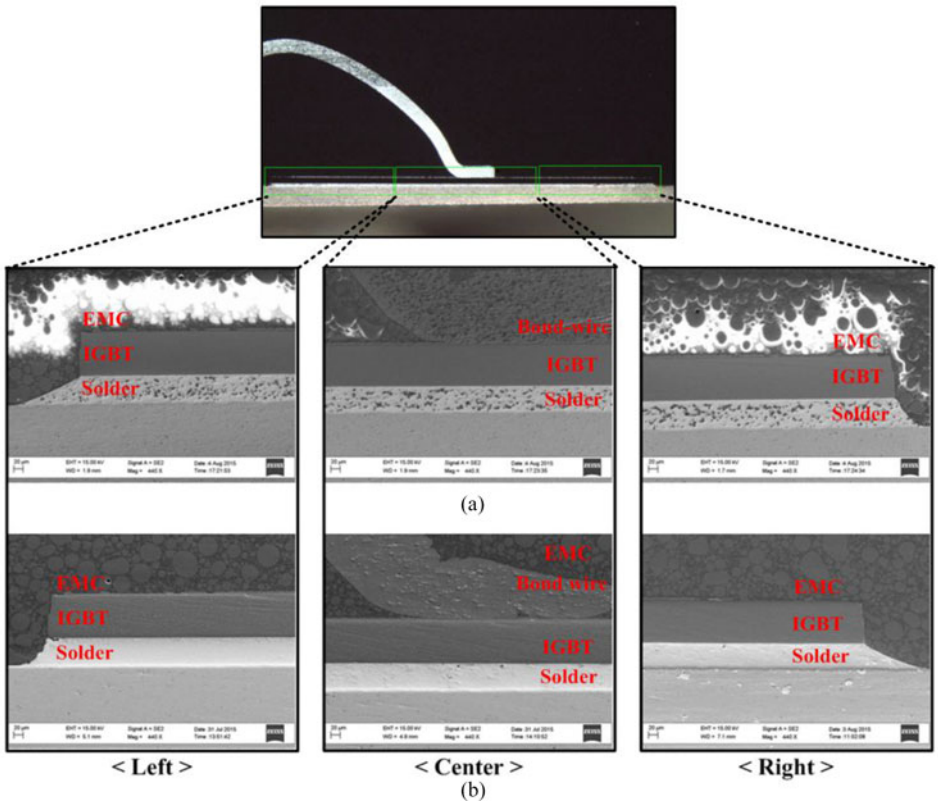

Fig. 12. SEM images of cross sectioned IGBTs for failure analysis. (a) Power cycling test under the condition 4 (1 s). (b) Power cycling test under the condition 1 (10 s).

Table V shows the parameter values of the lifetime model (4) under different lifetime definitions.

The obtained model can be used together with the impact of other parameters such as junction temperature swing ($\triangle T_j$) and mean junction temperature ($T_{\rm jm}$). By including $t_{\triangle T j}$ effect, the lifetime estimation of the IGBT module regarding the temperature stress under given mission profiles of the power converters could be improved.

V. Failure Analysis of IGBT Modules

The failure analysis of the tested modules under the relatively long and short $t_{\triangle T j}$, 10 and 1 s, are performed, respectively.

Fig. 9 shows SEM image of the tested module after the test under the condition 4 (1 s).

Cracks are observed in all the bond wires of $T_{\rm VL}$, which is the first failed device among six IGBTs. The cracks in bond wires are also observed in another tested module under the same condition as shown in Fig. 10. Fig. 11 shows the SEM image of tested IGBT module under the condition 1 (10 s). It can be seen that all the bond wires of the degraded IGBT are also cracked.

Fig. 12(a) and (b) shows the SEM images of the cross sectioned IGBT modules after the power cycling tests under the conditions 4 (1 s) and 1 (10 s), respectively. In all three sections, there is no visible degradation in solder joint and interface between chip and bond wires after the power cycling tests under both conditions. The black spots in the solder joint shown in Fig. 12(a) are not the degradation due to power cycling test but remained material from the IGBT module such as diamond lapping film consisting of carbon (C).

Investigation of the tested modules with SAM is also performed in order to check the solder degradation in detail.

Fig. 13(a) shows the configuration of the tested IGBT module and Fig. 13(b)–(e) shows the SAM images of the IGBT modules before and after the tests under the conditions 4, 3, and 1, respectively. There are no visible solder degradations in the IGBT modules after the tests under the conditions 4, 3, and 1, as shown in Fig. 13(c)–(e), compared with the IGBT module before the test, as shown in Fig. 13(b).

It is worth to be noted that the white spots in the SAM results are not due to the degradation by the power cycling test but solder voids from manufacturing process.

It can be seen from the failure analysis results that the bond-wire crack is the predominant failure mechanism of the tested IGBT modules under the test conditions defined in Table II. It should be noted that the main failure mechanism of IGBT modules could be different depending on the different packaging technologies and temperature stress conditions. Further, there are no big differences in the dominant failure mechanism due to the different temperature swing duration in the defined ranges. However, the power cycling tests under different test conditions such as smaller temperature swing and longer temperature swing duration still need to be performed in order to study the effect of different temperature stress conditions on the failure mechanisms of the power IGBT module.

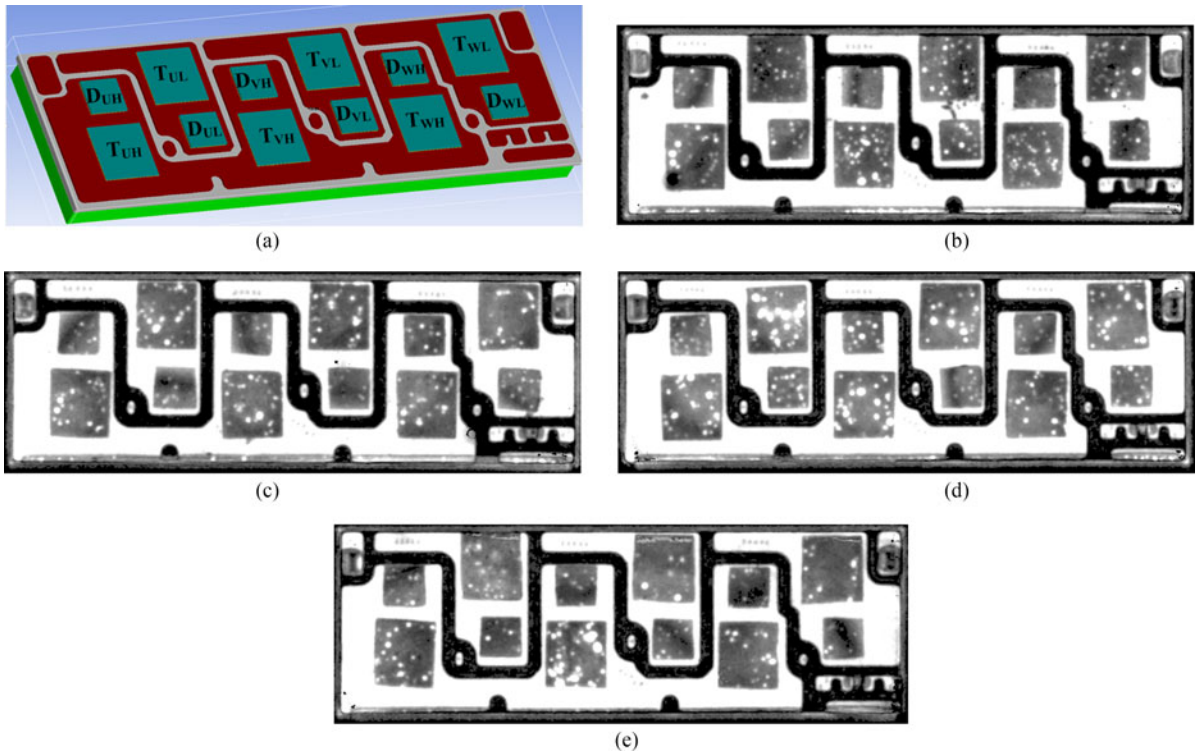

Fig. 13. SAM images of the IPM: (a) configuration of IPM, (b) before power cycling test, (c) after test under the condition 4 (1 s), (d) after test under the condition 3 (2 s), and (e) after test under the condition 1 (10 s).

VI. Conclusion

An effect of the junction temperature swing duration ($t_{\triangle Tj}$) on lifetime of IGBT modules has been studied with the advanced power cycling test setup. It can be seen from the result that $t_{\triangle Tj}$ has a significant effect on the lifetime. Further, test results show the importance of the statistical analysis for the lifetime modeling and reliability study.

The junction temperature swing duration dependent lifetime factor is also modeled based on a total of 39 accelerated power cycling test results under six different duration conditions. The different lifetime factors have been obtained for the specific type of the IGBT module under test with different definitions and confidence levels of a specific lifetime. The result shows the importance of the information about definition and confidence level for lifetime modeling. This study enables to include the effect of junction temperature swing duration on lifetime modeling and estimation of IGBT modules and it may result in improved lifetime prediction of IGBT modules under given mission profiles of power converters.

Finally, the postfailure analysis has been conducted to investigate the failure mechanism of the tested IGBT modules. The bond-wire cracks are observed in all tested modules and there are no visible degradation in the chip solder joint. Therefore, the bond-wire degradation is the predominant failure mechanism in the tested modules under the conditions that are performed. However, the power cycling tests under more various temperature stress conditions such as smaller temperature swing and longer temperature swing duration with a number of samples per condition still need to be performed in order to investigate the effect of temperature stress conditions on the failure mechanisms of the power IGBT module with statistic results.

References

[1] H. Wang *et al.*, "Transitioning to physics-of-failure as a reliability driver in power electronics," *IEEE J. Emerg. Sel. Topics Power Electron.*, vol. 2, no. 1, pp. 97–114, Mar. 2014.

[2] S. Yang, A. Bryant, P. Mawby, D. Xiang, L. Ran, and P. Tavner, "An industry-based survey of reliability in power electronic converters," *IEEE Trans. Ind. Appl.*, vol. 47, no. 3, pp. 1441–1451, May/Jun. 2011.

[3] U. M. Choi, F. Blaabjerg, and K. B. Lee, "Study and handling methods of power IGBT module failures in power electronic converter systems," *IEEE Trans. Power Electron.*, vol. 30, no. 5, pp. 2517–2533, May 2015.

[4] A. Volke and M. Hornkamp, *IGBT Modules: Technologies, Driver and Application*. Munich, Germany: Infineon Technologies A.G., 2011.

[5] M. Ciappa, "Selected failure mechanism of modern power modules," *Microelectron. Reliab.*, vol. 42, no. 4–5, pp. 653–667, Apr./May 2002.

[6] J. Lutz, H. Schlangenotto, U. Scheuermann, and R. D. Doncker, *Semiconductor Power Device*. New York, NY, USA: Springer-Verlag, 2011, ch. 11.

[7] H. S.-H. Chung, H. Wang, F. Blaabjerg, and M. Pecht, *Reliability of Power Electronic Converter Systems*. London, U.K.: The Institution of Engineering and Technology, 2016, ch. 9.

[8] E. Ozkol, F. Brem, C. Liu S. Hartmann, and A. Kopta, "Enhanced power cycling performance of IGBT modules with a reinforced emitter contact," *Microelectron. Reliab.*, vol. 55, no. 6, pp. 912–918, May 2015.

[9] V. Smet *et al.*, "Ageing and failure modes of IGBT modules in high-temperature cycling," *IEEE Trans. Ind. Electron.*, vol. 58, no. 10, pp. 4931–4941, Oct. 2011.

[10] K. Ma, M. Liserre, F. Blaabjerg, and T. Kerekes, "Thermal loading and lifetime estimation for power device considering mission profiles in wind power converter," *IEEE Trans. Power Electron.*, vol. 30, no. 2, pp. 590–602, Feb. 2015.

[11] H. S.-H. Chung, H. Wang, F. Blaabjerg, and M. Pecht, *Reliability of Power Electronic Converter Systems*. London, U.K.: The Institution of Engineering and Technology, 2016, ch. 5.
[12] U. M. Choi, S. Jørgensen, and F. Blaabjerg, "Advanced accelerated power cycling test for reliability investigation of power device modules," *IEEE Trans. Power Electron.*, vol. 31, no. 12, pp. 8371–8386, Dec. 2016.
[13] M. Held, P. Jacob, G. Nicoletti, P. Scacco, and M.-H. Poech, "Fast power cycling test of IGBT modules in traction application," *Int. J. Electron.*, vol. 86, no. 10, pp. 1193–1204, 1999.
[14] M. Ciappa, F. Carbognani, P. Cova, and W. Fichtner, "A novel thermomechanics-based lifetime prediction model for cycle fatigue failure mechanisms in power semiconductors," *Microelectron. Reliab.*, vol. 42, no. 9–11, pp. 1653–1658, Sep.–Nov. 2002.
[15] U. Scheuermann and R. Schmidt, "A new lifetime model for advanced power modules with sintered chips and optimized Al wire bonds," in *Proc. Conf. Power Convers. Intell. Motion Eur. 2013*, May 2013, pp. 810–817.
[16] U. Scheuermann and R. Schmidt, "Impact of load pulse duration on power cycling lifetime of Al wire bonds," *Microelectron. Reliab.*, vol. 53, no. 9–11, pp. 1687–1691, Sep.–Nov. 2013.
[17] R. Bayerer, T. Herrmann, T. Licht, J. Lutz, and M. Feller, "Model for power cycling lifetime of IGBT modules—Various factors influencing lifetime," in *Proc. 5th Int. Conf. Integr. Power Syst.*, Mar. 2008, pp. 1–6.
[18] P. O'Connor and A. Kleyner, *Practical Reliability Engineering*, 5th ed. Hoboken, NJ, USA: Wiley, 2012, ch. 3.
[19] J. Pippola, I. Vaalasranta, T. Marttila, J. Kiilunen, and L. Frisk, "Product level accelerated reliability testing of motor drives with input power interruptions," *IEEE Trans. Power Electron.*, vol. 30, no. 5, pp. 2614–2622, May 2015.
[20] ReliaSoft Corporation, Weibull++: Life data analysis software tool. [Online]. Available: http://www.reliasoft.com/Weibull/index.htm
[21] U. M. Choi, F. Blaabjerg, and S. Jørgensen, "Effect of junction temperature swing durations on a lifetime of a transfer molded IGBT module," in *Proc. Conf. Rec. ECCE 2016*, Sep. 2016, pp. 1–7.
[22] L. A. Escobar and W. Q. Meeker, "A review of accelerated test models," *Statist. Sci.*, vol. 21, no. 4, pp. 552–577, 2006.
[23] U. M. Choi, F. Blaabjerg, S. Munk-Nielsen, S. Jorgensen, and B. Rannestad, "Condition monitoring of IGBT module for reliability improvement of power converters," in *Proc. IEEE Conf. Expo Transp. Electrific. Asia-Pac. 2016*, Jun. 2016, pp. 602–607.

Ui-Min Choi (S'11–M'16) received the B.S. and M.S. degrees in electrical and computer engineering from Ajou University, Suwon, South Korea, and the Ph.D. degree in electrical engineering from Aalborg University, Aalborg, Denmark, in 2011, 2013, and 2016, respectively.

He is currently with the Department of Energy Technology, Aalborg University, as a Postdoctoral Researcher. His research interests include reliability of power device and converter, renewable power generation, and multilevel converter.

Frede Blaabjerg (S'86–M'88–SM'97–F'03) received the Ph.D. degree in electrical engineering from Aalborg University, Aalborg, Denmark, in 1992.

From 1987 to 1988, he was with the ABB-Scandia, Randers, Denmark. He became an Assistant Professor in 1992, an Associate Professor in 1996, and a Full Professor in power electronics and drives in 1998. He has been a Part-Time Research Leader in the Research Center Risoe. From 2006 to 2010, he was the Dean of the Faculty of Engineering, Science and Medicine and became Visiting Professor at Zhejiang University, Hangzhou, China, in 2009. His research interests include power electronics and its applications such as in wind turbines, PV systems, reliability, harmonics, and adjustable speed drives.

Dr. Blaabjerg was an Editor-in-Chief of the IEEE TRANSACTIONS ON POWER ELECTRONICS 2006–2012. He was a Distinguished Lecturer of the IEEE Power Electronics Society 2005–2007, and of the IEEE Industry Applications Society from 2010 to 2011. He has been the Chairman of EPE in 2007, and PEDG, Aalborg, Denmark, in 2012. He received the 1995 Angelos Award for his contribution in modulation technique and the Annual Teacher Prize at Aalborg University. In 1998, he received the Outstanding Young Power Electronics Engineer Award from the IEEE Power Electronics Society. He has received 15 IEEE Prize Paper awards and another Prize Paper Award in PELINCEC, Poland, in 2005. He received the IEEE PELS Distinguished Service Award in 2009, and the EPE-PEMC 2010 Council Award and the IEEE William E. Newell Power Electronics Award 2014. He has received a number of major research awards in Denmark.

Søren Jørgensen received the B.S. degree in electrical, electronic, and computer engineering from School of Engineering, Aarhus University, Aarhus, Denmark, in 2004.

Since 2012, he has been with the Grundfos Holding A/S, Bjerringbro, Denmark, where he is a Development Engineer in Grundfos Research and Technology, working with power semiconductor technology.